The Potential of Zero Total Charge and Electrocatalytic Properties of Ru@Pt Core-Shell Nanoparticles

Jørgen Svendby

Department of Materials Science and Engineering, Norwegian University of Science and Technology (NTNU), NO-7491 Trondheim, Norway.

Frode Seland

Department of Materials Science and Engineering, Norwegian University of Science and Technology (NTNU), NO-7491 Trondheim, Norway.

Gurvinder Singh

Department of Materials Science and Engineering, Norwegian University of Science and Technology (NTNU), NO-7491 Trondheim, Norway.

José Luis Gómez de la Fuente

Grupo de Química y Energías Sostenibles, Instituto de Catálisis y Petroleoquímica (CSIC), C/Marie Curie 2, L10, 28049 Madrid, Spain.

Svein Sunde[1,*]

Department of Materials Science and Engineering, Norwegian University of Science and Technology (NTNU), NO-7491 Trondheim, Norway.

Abstract

Electrocatalysis of the oxygen reduction reaction (ORR), oxidation of carbon monoxide, and the methanol oxidation reaction (MOR) are all critical to the performance of direct-methanol fuel cells (DMFC). In this work we analysed the activity and mechanism for these reactions at carbon-supported Ru@Pt core-shell catalysts based on measurements of the potential of zero total charge (PZTC) and cyclic voltammetry. The PZTC measured at Ru@Pt is approximately 140 mV lower than at Pt. An analysis of charging curves and complex-capacitance data shows that the lower PZTC cannot be explained exclusively by a lower potential of zero free charge (PZFC). The lower PZTC at the core-shell catalyst therefore indicates that OH adsorbs more strongly on the Ru@Pt than on Pt. From a scaling relation between the free energies of adsorbed oxygen and OH we infer that the lower PZTC value for Ru@Pt implies a larger potential-determining step for the ORR at this catalyst than at Pt. For oxidation of CO and the MOR the stronger binding of OH to the surface at Ru@Pt than at Pt is expected to increase the activity of the former. These predictions are in agreement with the results of measurements of the catalytic activity of the catalysts, and serve to rationalise the catalytic activity of Ru@Pt with respect to those of Pt for these reactions.

Keywords: electrocatalysis, PZTC, methanol oxidation reaction, CO oxidation, ORR
2010 MSC: 00-01, 99-00

1. Introduction

Electrocatalysis is important in energy-demanding industrial processes such as electrowinning and the chlor-alkali industries, and in electrochemical energy storage and conversion such as fuel cells and water electrolysis [1, 2]. Rational design of transition-metal catalysts for these applications is facilitated by the so-called d-band theory, which suggests that the binding energies of reaction intermediates depend primarily on the energy centre of the catalyst's d-band, i.e. the first moment of its density of states [3]. The binding energies of these intermediates are key to catalytic activity [4, 5, 6, 7, 8]. In other words, the d-band theory suggests that control

*Corresponding author. Tel.: +47 735 94051; fax: +47 73 59 11 05

Email address: svein.sunde@ntnu.no (Svein Sunde)

[1]ISE member

over the catalyst's d-band energy implies control over the catalytic activity.

One way to engineer the catalytic properties of a transition metal through tuning of its d-band energy is to deposit metal as an overlayer at another transition metal. This is expected to lead to either a lowering or raising of the d-band energy (depending also on band-filling) [3, 9, 10, 11, 12] through lattice strain [13] in the overlayer and through electronic interaction between the overlayer and the substrate [14]. For example, for a Pt monolayer on a Ru substrate, the shift in the d-band centre is estimated to more than half an electronvolt downwards with respect to that of bulk Pt [11]. Thus, CO-stripping peak potentials for Ru@Pt core-shell nanoparticles appearing at some 200 mV lower than those for Pt-nanoparticles of approximately the same size have been interpreted as due to a weakening of the CO-bond to the surface of the Ru@Pt/C relative to Pt/C [15, 16] in line with the experimental and theoretical results of Davies et al. [17]. Similarly, the oxygen bond is also weaker at Pt overlayers than at Pt [18, 19, 20, 21], the weaker the smaller the number of Pt monolayers on the Ru [18, 19].

The surface atom to which the adsorbate bonds [22] and therefore particle size [18, 23] also have a decisive effect on the binding energies of adsorbates. Whereas the d-band theory has been largely based on density-functional theory (DFT) calculations for well-defined step-free or low-index crystal surfaces, such calculations have shown more recently that the coordination number of the surface atom to which the adsorbate bonds also has a decisive effect on the binding energies. Thus, lowering the coordination number leads to stronger binding [22]. A second parameter that can be tuned to optimise catalytic activity is therefore the coordination number of the catalytic site. For catalysts consisting of nanoparticles this may be brought about by changing the particle size [23, 18], since small particles have more low-coordination sites (apices, edges and high-index surfaces) than larger particles or low-index bulk surfaces. Therefore, although Pt overlayers on Ru, Ir, and Rh overshoots the weakening of the OH binding energy with respect to that desirable for optimum ORR activity, it is possible to "climb" up the ORR volcano curve by introducing such undersaturated corner and edge sites [24].

Finally, the type of crystallographic planes will display different adsorption properties, and therefore different catalytic activity. For example, whereas the potential region for hydrogen adsorption is well separated from that for OH adsorption for Pt(111), these two potential regions partially overlap for Pt(100) [25]. Kinoshita [26, 27] suggested that a dependence of catalytic activity on particle size is related to changes in the relative fractions of effects on catalytic activities to be related to how the relative size of the various crystallographic planes and edge and corner sites vary with particle size. For core-shell particles one may expect similar particle-size effects, for example variations in the crystallographic planes for the core to propagate to the shell.

For Ru@Pt core-shell electrocatalysts [15, 16, 20, 28] it follows that core size and shape and shell thickness, parameters that will depend critically on synthesis method and conditions, will be decisive in determining their (electro-) catalytic properties. In principle the combined effects of these parameters may be addressed through DFT calculations, but this would assume knowledge of minute details of the catalytic sites which frequently remain experimentally inaccessible. It is therefore desirable to develop simple methods that can assess the binding energy of adsorbates in support of rationalising catalytic properties, analogous for example to those developed for addressing catalyst surface structure by CO-stripping [15, 29].

Previous work indicates that the potential of zero total charge (PZTC), a quantity which is accessible through quite simple experimental means, might provide such a method. For example, a correlation between catalytic activity for electrooxidation of carbon monoxide, for the oxygen reduction reaction (ORR), and the PZTC was demonstrated by Mayrhofer et al. [30] for Pt/C catalysts as a function of particle size. Similarly, Feliu et al. [31] showed that the PZTC is very sensitive to the number of steps at high-index surfaces, as is the electrocatalytic activity.

The PZTC is defined as the potential at which a change in surface area leads to no flow of charge [32, 33]. The flow of charge during such an area expansion, for solid electrodes often approximated by displacement of electrode charge by adsorption of a strongly adsorbing species such as CO [32, 34, 35, 36, 37], is

$$Q_{\mathrm{d}} = \sigma - \sum_k n_k F \Gamma_k. \qquad (1)$$

In this equation the first term on the right-hand side (σ) is the free electron charge at the electrode surface, which is zero at the potential of zero free charge (PZFC) [35, 38, 39]. The second term on the right-hand side of Eq. (1) [34, 35, 36] sums up the contribution to the charge due to species whose adsorption involves charge transfer, and n_k is the (signed) number of electrons transferred to the electrode during adsorption of

species k, Γ_k its surface excess, and F the Faraday constant. Q_d is a measurable quantity and is zero at the PZTC-potential value. Apparently, an analysis of the last two terms in Eq. (1) for an electrocatalyst would provide information on the binding of adsorbates to the electrocatalyst surface. This would be particularly convenient for adsorbates such as hydroxyl which are difficult to study by spectroscopic means.

In this paper we report the PZTC for Ru@Pt core-shell catalysts of size 3 – 4 nm loaded on Vulcan XC-72 support in a 0.1 mol dm^{-3} $HClO_4$-solution and in a 0.5 mol dm^{-3} H_2SO_4-solution. Based on the PZTC values and supported by an analysis of cyclic voltammograms and complex capacitance data we interpret and correlate kinetic data for the ORR, and MOR, and the electrooxidation of CO at Ru@Pt/C [4, 5, 6, 7, 8] in terms of binding energy of OH on Ru@Pt.

2. Experimental

Pt/C (HiSPEC® 3000, 20 wt% loading), PtRu/C (HiSPEC® 5000, 20 wt% Pt loading and 10 wt% Ru loading), both delivered from Alfa Aesar, and Ru@Pt/C (1:1 Pt/Ru ratio, 18 wt% loading) were used. All three catalysts had a mean diameter of 3 – 4 nm.

The Ru@Pt/C was prepared using the polyol synthesis method, based on the procedure of Alayoglu et al. [20, 28] and by our group [15]. Ruthenium(III)acetylacetonate ($Ru(Acac)_3$) and $PtCl_2$ (both from Alfa Aesar) were used as precursor for Ru and Pt, respectively. $Ru(Acac)_3$ was dissolved in ethylene glycol with the addition of polyvinylpyrrolidone (PVP, average MW = 58,000) to prevent agglomeration. Under an inert atmosphere the solution was heated up (2 °C/min) to 200 °C and kept there for 3 hours to reduce $Ru(Acac)_3$. After cooling down the solution the Ru nanoparticles were then coated by Pt atoms by mixing an already prepared ethylene glycol solution containing dissolved $PtCl_2$ and heating it up at a 2 °C/min rate to 170 °C followed by a 1 °C/min rate to 200 °C, and kept there for 75 minutes. After cooling down the solution, presonicated ethylene glycol containing Vulcan XC-72 was added to the solution. The solution was finally diluted with ethanol and centrifuged to dissolve and remove the PVP. The catalyst particles were dried in a heating cabinet and ground to a fine powder before use. The results of extensive structural and electrochemical characterisation have been reported elsewhere, not to be repeated extensively here, and thoroughly demonstrates the core-shell nature of these catalysts [15, 16, 20, 28], although high-resolution (HR) transmission electron microscopy (TEM) images obtained with a field emission JEOL 2100F instrument operating at 200kV will be presented.

All the electrochemical measurements were conducted in a conventional glass cell at a temperature of 22 ± 1 °C. The working electrode was a polished glassy carbon rotating disc electrode (RDE) from Pine Instruments (AFE3T050GC, 5 mm diameter, 0.196 cm^2 geometrical area). A reversible hydrogen electrode (RHE) was used as the reference, and a Pt-foil as the counter electrode. The electrolyte used was almost exclusively a 0.1 mol dm^{-3} $HClO_4$-solution prepared by dilution of concentrated $HClO_4$ in Milli-Q water (18.2 $M\Omega \cdot cm$). A 0.5 mol dm^{-3} H_2SO_4-solution prepared in the same manner was only used in the measurement of the PZTC in addition to the $HClO_4$-solution. The measurements were performed with a PGSTAT302N bipotentiostat from Autolab equipped with an analog Scan 250 sweep generator. The analog scan generator was used in all voltammetry reported here. Electrochemical impedance spectroscopy was performed from 100 kHz to 0.01 Hz at an amplitude of 0.01 V_{rms}.

The preparation procedure regarding the deposition of the catalysts on the RDE used, was based on the procedure reported by Garsany and coworkers [40, 41]. 1 ml of ink was prepared containing 0.2 ml concentrated isopropanol, 0.8 ml Milli-Q water, 20 μl Nafion ionomer solution (Alfa Aesar, 5 wt%), and sufficient catalyst powder to ensure a loading of 20 $\mu g_{Pt}/cm^2$. After 30 minutes of sonication, a 10 μl droplet was deposited on the glassy carbon disc and dried under a N_2-atmosphere. After the electrode was installed in the cell setup, cyclic sweeps at 100 mV/s and 10 mV/s between 0.05 V and 1.0 V (1.03 V for the ORR) were performed in an already Ar-purged solution until stable voltammograms were recorded.

The PZTC was measured using the CO-charge displacement technique [34, 42]. The current was measured during the constant potential values from 0.10 V – 0.18 V in random order and with an electrode rotation of 1000 rpm. The solutions were thoroughly purged with Ar for deaeration prior to the measurements. When the current had stabilised after 300 s, CO (purity 4.7, Linde) was introduced to the solution. After the current value had stabilised, the solution was purged with Ar for 30 minutes followed by cyclic sweeps to oxidise adsorbed CO. The procedure was then repeated for another potential value.

For the CO-stripping measurements, CO was bubbled into the solution for 10 minutes, followed by Ar purging for 30 minutes while the potential was kept at 0.05 V the whole time. Cyclic sweeps from 0.05 V to 1.0 V at 10

mV/s were then recorded.

The ORR measurement procedure was based on the work of Garsany et al. [40, 41]. It was done by cyclic sweeps at 20 mV/s between 1.03 V and 0.05 V with constant O_2-bubbling (purity 5.0, AGA), and an electrode rotation of 1600 rpm until a stable voltammogram was recorded, ensuring oxygen saturation. In addition, the capacitive- (background) and iR-contributions were measured based on the procedure reported by van der Vliet et al. [43] and used to correct the final ORR plots reported in this paper. The capacitive contribution was determined by recording stable cyclic voltammograms between 0.05 V and 1.03 V at 20 mV/s in an Ar-purged solution. The iR-contribution was determined by electrochemical impedance spectroscopy measurement from 10 kHz to 1 Hz at an amplitude of 0.01 V_{rms} and an electrode rotation of 1600 rpm.

For the CO-bulk measurements, the electrolyte was first purged with CO for 10 minutes at a constant electrode potential of 0.05 V. This was followed by cyclic sweeps at 10 mV/s between 0.05 V and 1.0 V with constant CO-bubbling at electrode rotations of 400, 625, 900, 1600, or 2500 rpm, performed in random order, until a stable voltammogram was recorded.

The methanol oxidation measurements were done by adding methanol (to give concentrations of 10^{-2} mol dm^{-3}, 10^{-1} mol dm^{-3}, 1.0 mol dm^{-3}, and 2.0 mol dm^{-3}) to the electrolyte solution under stirring before the given measurement to ensure a homogeneous solution. The potential was first kept at 0.05 V for 400 s before it was stepped up to either 0.4 V, 0.5 V or 0.6 V and kept at that potential for 1 h. Afterwards, the procedure was repeated where the potential was stepped up to one of the other potential values. After measuring the current at all three potential values, the methanol concentration was changed, and the procedure was repeated.

3. Results

Fig. 1 shows TEM images of the catalysts synthesised. Particles of approximately 4 nm across appear to dominate. Previous investigations of these catalysts have clearly demonstrated their core-shell nature through CO-stripping measurements, mapping of composition-profiles across individual particles, EXAFS analysis, and more [15, 16, 20, 28].

CO-charge displacement measurements in 0.1 mol dm^{-3} $HClO_4$ showed a significant difference between Ru@Pt/C and Pt/C. For Ru@Pt/C the charge through the electrode was positive below 0.14 V and negative above. Hence the PZTC is 0.14 V for

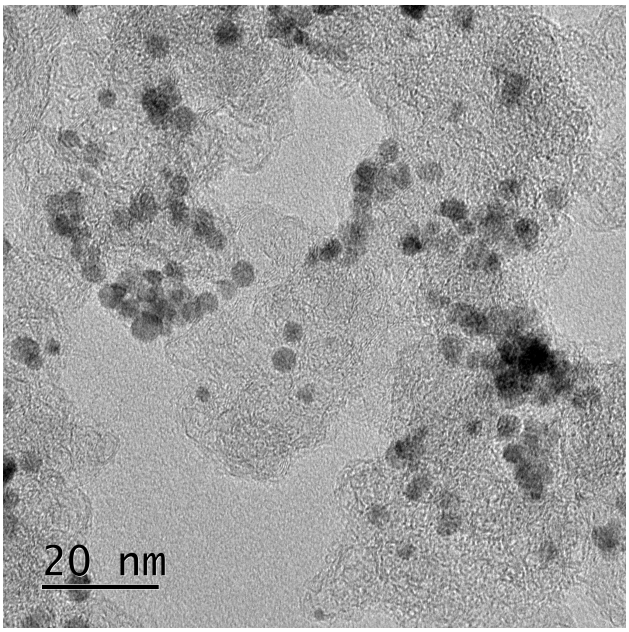

(a)

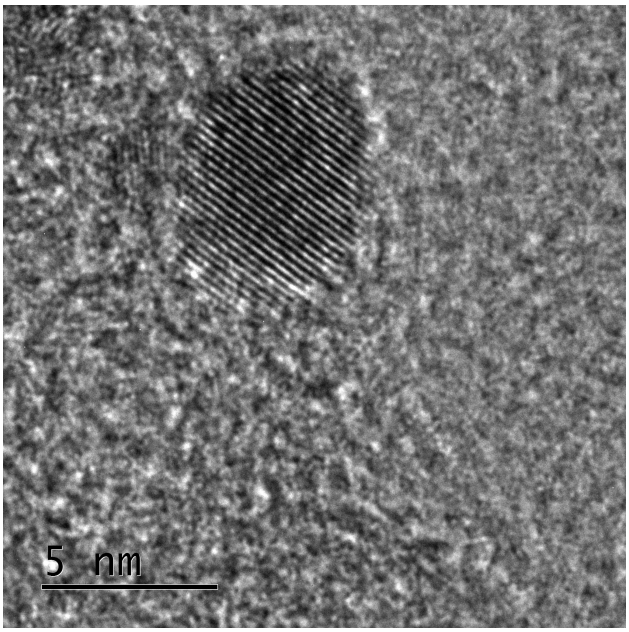

(b)

Figure 1: (1(a)) TEM image of Ru@Pt particles deposited on carbon. (1(b)) TEM image of a single Ru@Pt particle on carbon.

Ru@Pt/C. Details are given in the Electronic Supplementary Information. Similar measurements for Pt particles of similar size on carbon have shown that the charge through the electrode is positive below approximately 0.27 V or a little less than this, and negative above this potential [30, 44]. We will assume a value for the PZTC for Pt/C of 0.27 V below. For PtRu alloys Jeon et al. [45] found a PZTC of 0.042 V vs. RHE in 0.1 mol dm^{-3} $HClO_4$ solutions. The PZTC for Ru@Pt thus lies between the reported PZTC-values for Pt/C and PtRu/C.

CO-charge displacement measurements in 0.5 mol dm^{-3} H_2SO_4 also showed a significant difference between Ru@Pt/C and values reported for Pt [32] (in sulfuric acid). For Ru@Pt/C the charge through the electrode was positive below approximately 0.16 V and negative above. Hence the PZTC is 0.16 V for Ru@Pt/C in 0.5 mol dm^{-3} H_2SO_4. Details are given in the Electronic Supplementary Information.

Fig. 2 shows cyclic voltammograms (CVs) of the Pt catalyst (above) and the Ru@Pt core-shell catalyst (below) in 0.1 mol dm^{-3} $HClO_4$ at a sweep rate of 10 mV s^{-1}. These CVs are similar to those previously recorded by Tsypkin et al. [16], Bernechea et al. [46], Yang et al. [19], Chen et al. [47], and Jackson et al. [48] for Ru@Pt core-shell catalysts. Whereas the CV of Pt/C displays two clearly distinguishable peaks related to under-potential deposition of hydrogen (H_{UPD}) at approximately 0.2 V and below, as is typical for such catalysts [49], the corresponding region for the Ru@Pt catalyst shows considerably less structure. The CO-normalised charge subtracted for the apparent background current is much larger for the Pt catalyst than for the Ru@Pt catalyst (see Supplementary Material for information). However, the H_{UPD} region appears to span the same potential region at both catalysts. Finally, the currents in the potential range just positive of the H_{UPD} regions are relatively much larger at the Ru@Pt/C than for the Pt/C catalyst.

We have included in Fig. 2 also the anodic part of the voltammetric charge as obtained by integration from the PZTC to various potentials according to [25, 50, 51, 52, 53]

$$Q_{CV}(E) = \int_{E_{PZTC}}^{E} \frac{j}{\nu} dE \qquad (2)$$

Both for the measurements in $HClO_4$ and H_2SO_4 the agreement between the displacement charges and those found from Eq. (2) were in very good agreement, see Electronic Supplementary Information for a comparison.

The apparently linear relation between charge and

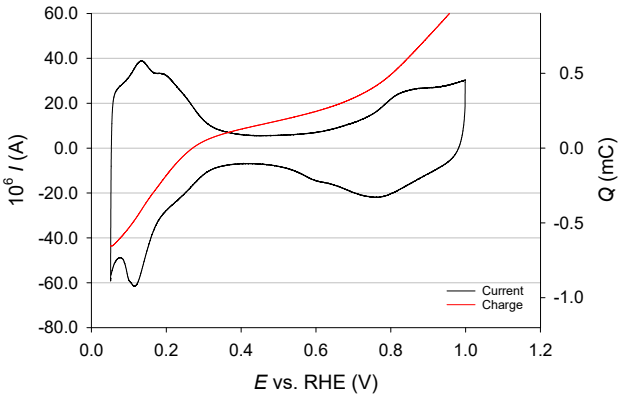

(a)

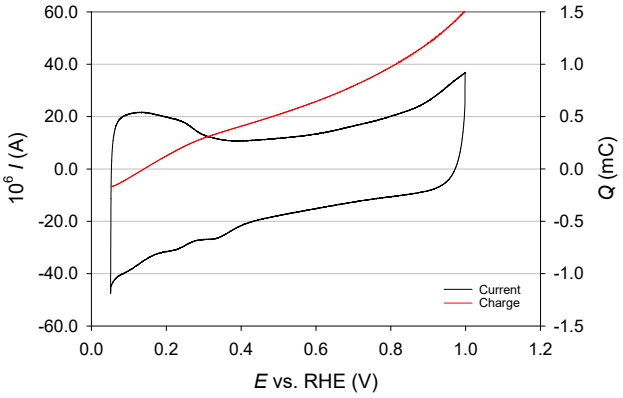

(b)

Figure 2: 2(a) Cyclic voltammogram of Pt/C in 0.1 mol dm^{-3} $HClO_4$(aq) at a sweep rate of 10 mV s^{-1}, 2(b) Cyclic voltammogram of Ru@Pt/C in 0.1 mol dm^{-3} $HClO_4$(aq) at a sweep rate of 10 mV s^{-1}. The voltammetric charge Q_{CV} as calculated from Eq. (2) is shown for both voltammograms.

potential between approximately 0.35 V and 0.5 V in Fig. 2(a) extrapolates to zero charge at approximately 0.2 V. A similar extrapolation for the Ru@Pt catalyst gives approximately 0 V at zero charge. For electrodes with well separated hydrogen and hydroxyl adsorption the potential at which the extrapolated charge crosses the potential axis has sometimes been used in order to obtain an estimate for the PZFC [52, 53], frequently in good agreement with estimates for the maximum entropy potential. The condition that adsorption regions for hydrogen and OH are well separated is equivalent to assuming that any linear charge-potential relation in the intermediate potential region reflects double-layer charging.

From the perspective of catalytic properties the last term on the right-hand side of Eq. (1) is the most interesting. In order to verify that the differences observed in the PZTC here are indeed dominated by the adsorption properties of the catalysts and not by differences in the PZFC, we measured the impedance of Ru@Pt and Pt catalysts in oxygen-free $HClO_4$.

Fig. 3 shows a complex-plane plot for a Ru@Pt/C catalyst at 0.5 V vs. RHE in 0.1 mol dm^{-3} $HClO_4$. The complex capacitance is defined as $C = Y(j\omega)/j\omega$, where $Y(j\omega)$ is the admittance of the electrode [54]. The ohmic resistance was evaluated from the impedance-plane plot and subtracted from the data before calculating the complex capacitance. (The values for the ohmic resistance were in good agreement with that calculated from the formula for resistance to a disk [55, 56].) The complex capacitance for a capacitance C is independent of frequency and equal to C, which corresponds to a point in the complex-capacitance plane plot [54, p. 468]. A resistance in parallel with capacitance will result in a straight vertical line in a complex capacitance plot, whereas a resistance in series with a capacitance gives a semicircle in this representation. Fig. 3 therefore shows that the impedance of the Ru@Pt catalyst at 0.5 V contains at least one resistance in series with a capacitance in addition to the ohmic resistance. Furthermore, this resistance is shunted by a second capacitance; otherwise it would form a part of the apparent ohmic resistance. We therefore conclude that the equivalent circuit for the Ru@Pt/C electrode consist of at least an ohmic resistance in series with a parallel circuit consisting of a capacitance in one branch and a resistance and a capacitor in series in the other branch. An expanded discussion of this analysis is given in the Supplementary Material.

Fig. 4 shows the background- and iR-corrected negative going sweep of the ORR measurement for Pt/C, PtRu/C, and Ru@Pt/C with a current normalised with respect to either the geometrical a) or active b) (CO-based) surface areas. The measurement starts at 1.03 V, all at about the same current density. All samples have relatively close limiting current densities (j_l) in the low-potential region. As seen from plot a), all the j_l-values are within 10 % of the theoretical value 5.7 mA/cm$^2_{\text{Geo}}$ for the geometrical current density for an electrode rotation of 1600 rpm in an oxygen-saturated solution, which is considered necessary for a properly executed measurement [40, 57].

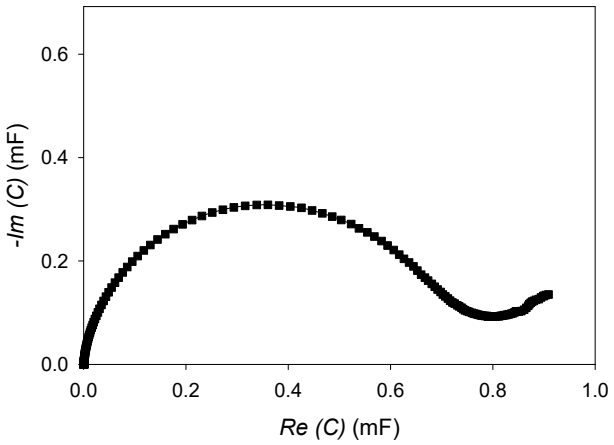

Figure 3: Complex capacitance plot of a Ru@Pt/C catalyst at 0.5 V vs. RHE in 0.1 mol dm^{-3} $HClO_4$. The ohmic resistance was evaluated from the corresponding impedance-plane plot and subtracted from the data before calculating the complex capacitance.

As can be seen, both PtRu/C and Ru@Pt/C have larger overpotentials than Pt/C, the overpotential of PtRu/C being only slightly larger than that of Ru@Pt/C. The onset potentials for PtRu/C and Ru@Pt/C are significantly larger, roughly 80 mV, compared to Pt/C and thus differ from those of Jackson et al. [18] whose Ru@Pt/C catalysts displayed much lesser difference in the onset potential.[2] Also, whereas our Ru@Pt/C catalysts have larger overpotentials for the ORR than Pt/C, those of Jackson et al. [18] are more, not less, efficient for the ORR. The Ru@Pt/C catalysts by Yang et al. [19], who reported ORR activity for Ru@Pt/C manufactured by galvanic displacement of Cu by Pt, displays both larger and smaller onset potentials than Pt/C depending on the number of Pt monolayers in the core-shell catalyst.

[2] We have defined onset potential in this work as the potential at which the current density value is 5 % of either the peak current density value (CO-stripping, CO-bulk, methanol oxidation) or the j_l (ORR).

We ascribe the differences between our catalysts and those reported elsewhere to the different synthesis procedures employed. The catalyst manufacured by Jackson et al. [18] included annealing at 300 °C. Tsypkin *et al.* [16] found that annealing changes bond lengths and the extent of alloying in Ru@Pt core-shell particles with accompanying and significant changes in the catalytic activity of the particles. Also, TEM images of the catalysts in Ref. [18] appear to indicate some particle agglomeration, which is also known to induce changes in catalytic activity [58, 59]. Yang *et al.* [19] found that the activity for the ORR was higher for two monolayers of Pt at Ru (manufactured by surface-limited redox replacement) than for three. Based on the measured extent of alloying we have previously estimated our Ru@Pt catalysts to contain approximately four monolayers. A lower activity in our catalysts is therefore reasonable. Also, the catalysts by Yang *et al.* [19] will not have complete shells, at least for the monolayer samples, since galvanic replacement of Cu with Pt^{2+} is not a 100% efficient process. (Our Ru@Pt catalysts do not show any signs of such surface ruthenium [15].) Finally, results of Price *et al.* [60] indicate that catalysts prepared by galvanic replacement form cluster of the deposited metal on the core rather than complete monolayers.

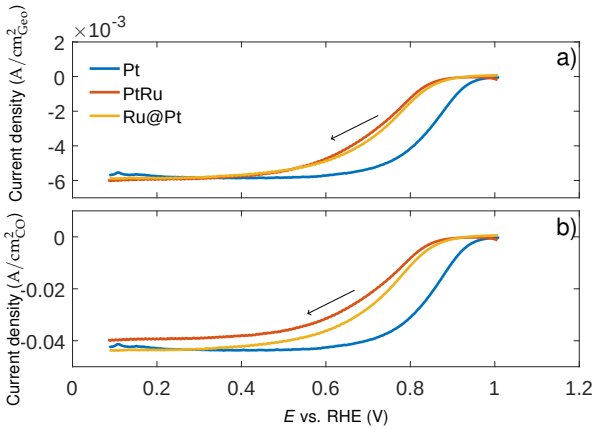

Figure 4: Currents in an oxygen-saturated solution of 0.1 mol dm^{-3} $HClO_4$ for Pt/C, PtRu/C, and Ru@Pt/C, 1.03 V → 0.05 V, 20 mV/s at 1600 rpm. Plot a) is normalised with respect to geometric area and plot b) with respect to active surface area (CO-based). Both plots are corrected for background- and iR-contributions.

The 80 mV onset potential difference is also reflected in Fig. 5 which shows Tafel plots for Pt/C, PtRu/C, and Ru@Pt/C, obtained from Fig. 4 b). The Tafel curves are not completely linear, which is rather typical for Pt-based nanostructured catalyst,[18, 30] but linear fits indicate slopes of 120 mV/dec, 160 mV/dec, and 140 mV/dec for Pt/C, PtRu/C, and Ru@Pt/C, respectively. For Pt, 120 mV/dec is reported for the high overpotential region (above 0.85 V vs. RHE), while 60 mV/dec is reported for the low overpotential region (below 0.85 V vs. RHE) [61]. For PtRu/C, the same slopes have been reported [62]. A clear-cut 60 mV slope was not observed here.

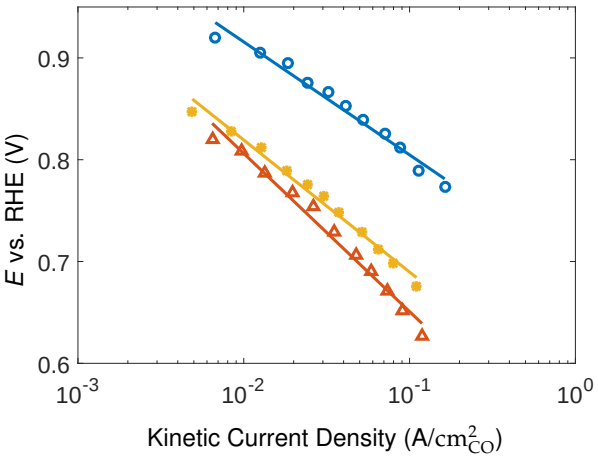

Figure 5: Tafel plot for the ORR for Pt/C (blue), PtRu/C (red), and Ru@Pt/C (yellow).

Fig. 6 shows the stripping voltammogram for the oxidation of a monolayer of CO for Pt/C, PtRu/C, and Ru@Pt/C. As seen, Pt/C has the highest overpotential for oxidising the CO-layer on its surface with a peak position at ca. 0.79 V, followed by Ru@Pt/C (ca. 0.57 V) and PtRu/C (ca. 0.51 V). This trend is in accordance with previous results [15, 63]. The stripping voltammogram indicates that the double layer capacitance is negligible for the electrode saturated with CO, as is an underlying assumption for setting the experimental displacement charge equal to Q_d in Eq. (1) [37, 52, 53].

Charge in CO-stripping voltammetry is assumed to be associated solely with the catalyst particles and not with the support. The large cathodic currents on the return sweep in Fig. 6 are the same as in the voltammogram in Fig. 2. However, the corresponding anodic currents are absent in the forward sweep of Fig. 6 since CO blocks the surface. This therefore shows that the currents in the intermediate potential region 0.4 V – 0.6 V in the voltammograms in Fig. 2 must be ascribed to the catalyst particles and not to the support.

Fig. 7 and 8 display current vs. voltage curves in 0.1 mol dm^{-3} $HClO_4$-solution for oxidation of dissolved CO at rotating disc electrodes with pre-deposited Pt/C and Ru@Pt/C catalysts with a sweep rate of 10 mV/s. In both cases the polarisation curves display substantial hysteresis, and a larger potential is required for

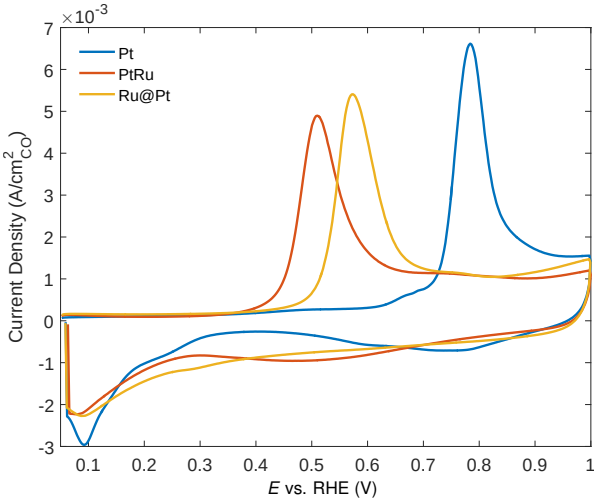

Figure 6: The first sweep of CO-stripping cyclic voltammetry at 10 mV/s between 0.05 V and 1.0 V in 0.1 mol dm^{-3} $HClO_4$ for Pt/C, PtRu/C, and Ru@Pt/C. Before the sweeps, CO gas was bubbled in the solution at a constant potential of 0.05 V for 10 minutes, followed by Ar-gas bubbling for 30 minutes at the same potential to remove the CO in the solution.

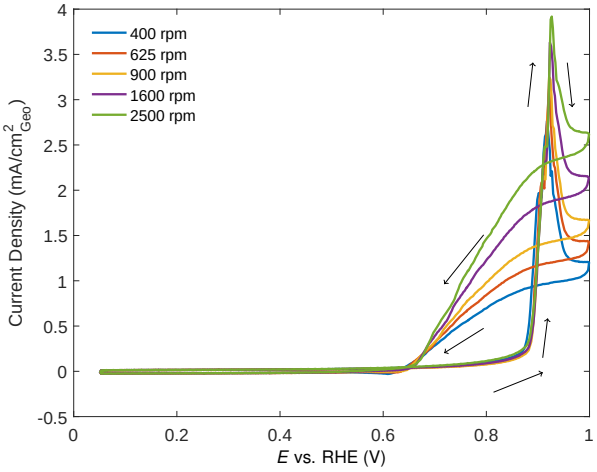

Figure 7: Oxidation of dissolved CO at Pt/C at a rotating disc electrode. Rotation rates are given in the legend. The potential was swept between 0.05 V and 1.0 V at a sweep rate of 10 mV/s in a 0.1 mol dm^{-3} $HClO_4$-solution.

the onset of the reaction in the positive-going sweep than the potential at which the reaction ceases in the negative-going sweep. For Pt/C the onset potential is around 0.85 V (in the positive-going sweep). In the negative-going sweep the current drops gradually and eventually ceases at around 0.65 V. For the Ru@Pt/C catalyst the corresponding numbers are 0.62 V and 0.48 V, respectively.[3] For Pt/C well-defined limiting currents are observed at potentials more positive than the current spike at potentials following the onset, and these limiting currents were found to comply well with the Levich equation, being proportional to $\omega^{1/2}$, where ω is the rotation angular frequency of the disc. For Ru@Pt/C, however, the current displays no stable limiting values at potentials positive of the spike, and continues to increase until a second peak emerges at the same potential as the spike observed at Pt/C.

The voltammograms in Fig. 7 and 8 comply quite well, apart from the extra current spike at higher potentials for Ru@Pt/C, to the shapes predicted by the model of Koper et al. [64]. According to this model the onset potential being higher than the peak in CO-stripping voltammograms is associated with the continuous adsorption of CO from the solution as CO is oxidised, thus leading to higher potentials being necessary to establish free sites at the surface necessary for the oxidation process. The hysteresis is related to the oxidation process being dependent on the state of the surface; in the negative-going sweep there is a balance between CO being oxidised and the influx of new CO-molecules by diffusion whereas in the positive-going sweep the surface will be covered with adsorbed CO.

Similar results were obtained at PtRu/C alloy catalysts, which showed onset potentials similar to those of Ru@Pt/C. However, for the alloy catalysts much more clearly defined limiting currents were observed, the polarization curves complying quite well with the shapes predicted by the model of Koper et al. [64].

The onset potentials for the MOR were determined from cyclic voltammograms (1 mV/s sweep rate and an electrode rotation of 900 rpm) in a 0.5 M H_2SO_4 + 1.0 M CH_3OH-solution (the MOR-measurements will be presented elsewhere) [65]. The onset potentials for the three catalysts from the different measurements presented here are listed in Table 1. All onset potentials decrease with decreasing PZTC. This corresponds to a lower activity of the ORR the lower the PZTC, and vice versa for the MOR and the CO-electrooxidation reactions.

The differences in the onset potential for the MOR are also reflected in the activity measured as the current in chronoamperometric measurements at high methanol concentration and low potential, Fig. 9. Since 0.6 V is right at the onset potential for Pt/C the rate of oxidation is very low and competes only successfully with adsorption of methanol at the lowest concentrations, hence the reduction in current at higher concentrations at which

[3]For the CO-bulk oxidation at Ru@Pt/C, the peak at the lowest potential value was used to define the onset potential for this reaction.

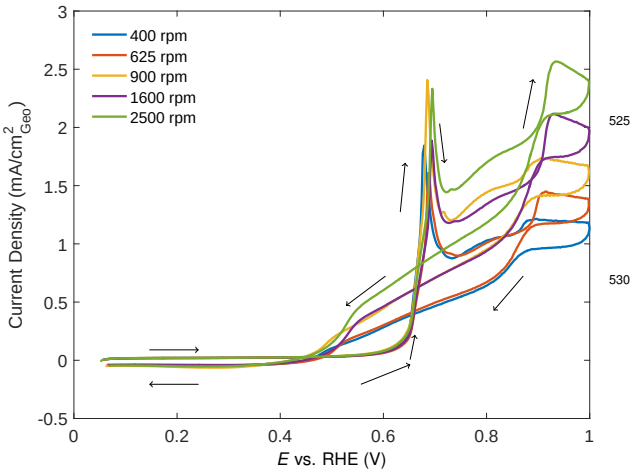

Figure 8: Oxidation of dissolved CO at Ru@Pt/C at a rotating disc electrode. Rotation rates are given in the legend. The potential was swept between 0.05 V and 1.0 V at a sweep rate of 10 mV/s in a 0.1 mol dm^{-3} $HClO_4$-solution.

Table 1: Onset potentials vs. RHE for the oxygen reduction reaction, CO-stripping, CO-bulk, and the methanol oxidation reaction. The PZTC-values obtained here for Ru@Pt/C and those for Pt/C [30] and PtRu/C [45] are included for comparison. (The onset potentials were estimated from linear plots, not logarithmic plots as in Ref. [66].)

	$E_{Pt/C}$ (V)	$E_{Ru@Pt/C}$ (V)	$E_{PtRu/C}$ (V)
ORR	0.95	0.87	0.86
$CO_{Stripping}$	0.62	0.43	0.38
CO_{Bulk}	0.85	0.62	-
MOR	0.60[65]	0.54[65]	0.50[65]
PZTC	0.27	0.14	0.04

the electrochemical reaction rates are too low to prevent the surface from filling up with adsorbed CO. For the other two electrodes 0.6 V is past the onset, and the higher rates of methanol adsorption at higher concentrations are paralleled by a higher MOR current.

4. Discussion

As argued above it is difficult to associate the complex capacitance data in Fig. 3 as due to a single double-layer charging process. The complex capacitance of the Ru@Pt/C (Fig. 3) as well as those of the Pt/C electrodes (not shown) actually correspond qualitatively to equivalent circuits derived for adsorption processes involving one or two adsorbates [67, 68]. We therefore interpret the results as involving faradaic adsorption at the electrode also in the pseudo-capacitive region. It is therefore not likely that the (pseudo-) capacitive region for the Ru-containing catalysts, including the Ru@Pt catalysts, can be extrapolated meaningfully to give the free charge as discussed in the Supplementary Material. Also, if the currents in the intermediate potential region 0.4 V – 0.6 V were to be interpreted as double layer charging they would imply that the double layer capacitance is more than five times higher for the Ru@Pt catalyst as normalised with respect to the hydrogen UPD charge. We consider this unlikely, and disregard the possibility that differences in the double-layer charge and the PZFC dominates the differences in the PZTC between Pt and Ru@Pt.

The significance of the lower PZTC for the Ru@Pt and the PtRu catalysts with respect to Pt is therefore that they imply a stronger binding of OH to the surface through the last term in Eq. (1), which we may expand on the assumption that adsorption of perchlorate species is negligible [69, 70] as [34]

$$Q_d(E) = -\sigma(E) + F\Gamma_H(E) - F\Gamma_{OH}(E) \qquad (3)$$

Displacement of hydrogen from the electrode surface by CO will give a positive displacement charge through the reaction

$$H_{ad} + CO(aq) \rightleftharpoons H^+(aq) + e^- + CO_{ad} \qquad (4)$$

whereas displacement of hydroxyl will give rise to a negative displacement charge through

$$OH_{ad} + CO(aq) + e^- \rightleftharpoons OH^-(aq) + CO_{ad} \qquad (5)$$

The stronger the hydrogen binds to the surface the higher the PZTC, i.e. the higher the potential required to desorb it and thus the higher the PZTC *ceterus paribus*. Vice versa, the stronger the OH binds to the surface the lower the PZTC, everything else being the same.

From Fig. 2 the potential for desorption of weakly adsorbed hydrogen appears to be approximately the same for Ru@Pt and Pt.The low PZTC of the Ru@Pt catalyst with respect to Pt suggests that the inferior activity for the ORR at the Ru@Pt catalyst is due to stronger binding of OH at the latter [30]. For example, for the reaction mechanism proposed by Nørskov and coworkers [5, 6] and with the use of the scaling relation between the binding energies of oxygen and OH, it is easy to show that a stronger binding of OH at the surface implies a lower onset potential for the ORR at Ru@Pt relative to Pt. See Supplementary Material for details.

In a similar fashion, it is also easy to show that the magnitude of the potential-determining step for the CO oxidation and methanol-oxidation reactions will decrease if the binding energy of OH increases [8, 4]. In these cases, the magnitude of the potential-determining step will also be determined by the binding energy of

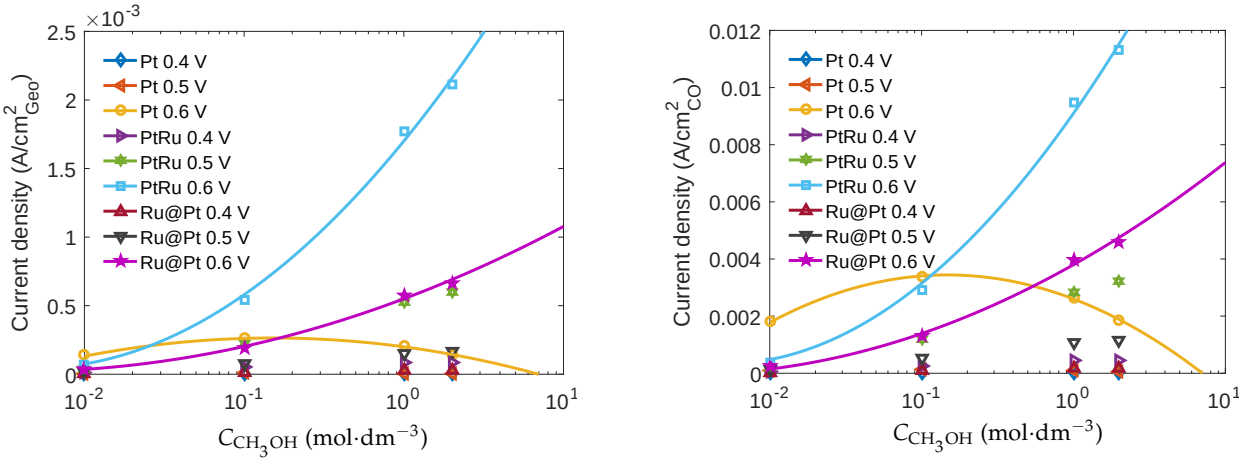

Figure 9: Current densities based on geometrical area (left) and active area from CO-stripping measurements (right) for Pt/C, PtRu/C, and Ru@Pt/C in 0.1 mol dm^{-3} $HClO_4$. The current density points plotted are the values taken after 1000 s of chronoamperometry at potentials between 0.4 V and 0.6 V at methanol concentrations between 10^{-2} mol dm^{-3} and 2 mol dm^{-3}. Curves showing the trends for the three catalysts at 0.6 V are included.

CO. However, a stronger binding of OH is consistent with the decrease in the onset potential observed in this work for these reactions at the Ru@Pt catalysts with respect to those of Pt. A similar argument for a correlation between the PZTC and catalytic activity for the ORR and CO oxidation for Pt catalysts of varying particle size was put forward by Mayrhofer *et al.* [30].

The PZTC, the voltammograms, and the activity for the reactions investigated here thus all appear to suggest that the binding energy of oxygen and OH at the Ru@Pt surface is stronger than at the Pt surface for catalysts of similar size. Strain is not a likely cause for these differences, since the Pt-Pt bond distance in Ru@Pt catalysts identical to those investigated here was found to be smaller than that of Pt by only less than 1%. Residual electronic coupling between the Ru core and the Pt shell, dominating for thin shells, is another possible reason for differences in the binding energy as discussed by Schlapka et al. [14] for adsorption of CO. However, both theory and experiment for monocrystalline model systems indicate that the Ru substrate would serve to decrease the binding energy of hydrogen [20, 71] and oxygen [19, 20, 72] at Pt overlayers with respect to bulk Pt, in contrast to what we conclude for the Ru@Pt catalysts above. We therefore consider a rearrangement of the catalyst surfaces as proposed by Kinoshita [26] possibly combined with the effects of sites of low coordination number to play a dominating role in changing the binding energy and thus catalyst activity for Pt on Ru as in the Ru@Pt core-shell catalysts investigated here.

If particle size effects are to explain the differences between Ru@Pt and Pt in their PZTC and electrocatalytic activity, particle-size effects for Ru@Pt cannot be the same as those for Pt. Kinoshita [26, 27] considered cubo-octahedral particles to represent the minimum surface energy for Pt particles. The quantitative relation between the different facets, edges and corners was then established through the analysis of van Hardeveld and Hartog [73]. Any catalysts for which the assumption of cubo-octahedral shape applies would then be expected to follow similar trends in terms of catalytic activity vs. particle size. However, the thermodynamically stable particle shape will depend the relative surface tensions of its crystal planes, as utilised in the Wulff construction [74, 75]. Therefore the equilibrium shape of a particle consisting of a platinum shell deposited on a preformed hexagonally close-packed ruthenium core may have a very different shape from that of a platinum particle. To the extent that the particle relaxes towards its equilibrium shape before or during characterisation, the shape will also depend on the interfacial energy between the Ru core and the Pt shell. In addition, kinetic factors during synthesis may lead to different morphologies when processing conditions are changed. In conclusion, therefore, particle effects such as those ascribed to low-coordinated sites will depend on chemical composition, catalyst architecture, and synthesis. We tentatively ascribe the findings here to such differences between Ru@Pt and Pt.

The stronger OH bond at Ru@Pt with respect to Pt, which is implied by the results reported above, is surprising since theoretical considerations suggest a weaker bond for Pt overlayers at Ru, as elaborated in the Introduction. Although strengthening of the bond

may be obtained by introducing low-coordination sites, what exists of theoretical calculations indicate that although the OH bond strength may approach that at Pt as such sites are introduced it will not surpass it [24].

The second peak for oxidation of dissolved CO at approximately 0.9 V in Fig. 8 appears to correspond to the oxidation peak for Pt in Fig. 7, which appears at approximately the same potential. This peak does not correspond to separate Pt particles or thick Pt protrusions in the Ru@Pt catalyst since this would be difficult to reconcile with the low onset potential for the ORR at this catalyst. If any such separate Pt regions existed in the Ru@Pt catalyst they should contribute to the onset potential for the ORR, which they do not. Also, there is little evidence of such catalyst heterogeneity in the CO stripping voltammograms. Still, these peaks suggest the existence of a heterogeneous catalytic activity for CO, of which the second process is related to the binding energy or kinetics for re-adsorption of CO in solutions of dissolved CO.

5. Conclusion

Measured PZTC-values for Ru@Pt/C, Pt/C and PtRu/C in perchloric acid demonstrates a correlation between the PZTC-value and the activity for oxidation of adsorbed and dissolved CO, for electrooxidation of methanol, and for the oxygen reduction reaction. A decreased PZTC-value is thus associated with an decreased activity for the oxygen reduction reaction, but higher activity for electrooxidation of CO and methanol.

Complex-capacitance data show that faradaic adsorption contributes to the pseudo-capacitive currents in the intermediate potential region from approximately 0.4 V through 0.6 V. Thus, the PZTC values cannot be rationalised as being due to a shift in the PZFC. The lower PZTC at the core-shell catalysts therefore implies a stronger binding of OH_{ad} at the catalyst surface. This explains the lower catalytic activity for the oxygen-reduction reaction at Ru@Pt, and will also contribute to the higher activity for methanol and CO oxidation.

Acknowledgements

The authors acknowledge the financial support from the Joint Research Center for Materials and New Energy between Shanghai Jiao Tong University and NTNU (financed by NTNU strategic funds, project no. 80354000) and from the Research Council of Norway's NANOMAT program, contract no 182044 "Oxidation of small organic molecules". The TEM work was carried out using NORTEM infrastructure, Grant 197405, TEM Gemini Centre, Norwegian University of Science and Technology (NTNU), Norway.

References

[1] W. Schmickler, E. Santos, Interfacial Electrochemistry, 2nd Edition, Springer, 2010.

[2] M. Koper, A. Wieckowski, Fuel Cell Catalysis, 1st Edition, John Wiley & Sons, 2009.

[3] B. Hammer, J. K. Nørskov, Theoretical Surface Science — Calculations and Concepts, Adv. Catal. 45 (2000) 71–129. doi:10.1016/S0360-0564(02)45013-4.

[4] P. Ferrin, A. U. Nilekar, J. Greeley, M. Mavrikakis, J. Rossmeisl, Reactivity descriptors for direct methanol fuel cell anode catalysts, Surf. Sci. 602 (21) (2008) 3424–3431. doi:10.1016/j.susc.2008.08.011.

[5] J. K. Nørskov, J. Rossmeisl, A. Logadóttir, L. Lindqvist, J. R. Kitchin, T. Bligaard, H. Jónsson, Origin of the Overpotential for Oxygen Reduction at a Fuel-Cell Cathode, J. Phys. Chem. B 108 (46) (2004) 17886–17892. doi:10.1021/jp047349j.

[6] J. Rossmeisl, A. Logadóttir, J. K. Nørskov, Electrolysis of water on (oxidized) metal surfaces, Chem. Phys. 319 (2005) 178–184. doi:10.1016/j.chemphys.2005.05.038.

[7] J. Rossmeisl, Z.-W. Qu, H. Zhu, G.-J. Kroes, J. K. Nørskov, Electrolysis of water on oxide surfaces, J. Electroanal. Chem. 607 (2007) 83–89. doi:10.1016/j.jelechem.2006.11.008.

[8] G. A. Tritsaris, J. Rossmeisl, Methanol Oxidation on Model Elemental and Bimetallic Transition Metal Surfaces, J. Phys. Chem. C 116 (22) (2012) 11980–11986. doi:10.1021/jp209506d.

[9] T. Bligaard, J. K. Nørskov, Ligand effects in heterogeneous catalysis and electrochemistry, Electrochim. Acta 52 (18) (2007) 5512–5516. doi:10.1016/j.electacta.2007.02.041.

[10] J. Ontaneda, R. A. Bennett, R. Grau-Crespo, Adsorption of methyl acetoacetate at Ni{111}: Experiment and theory, J. Phys. Chem. C 119 (41) (2015) 23436–23444. doi:10.1021/acs.jpcc.5b06070.

[11] A. Ruban, B. Hammer, P. Stoltze, H. L. Skriver, J. K. Nørskov, Surface electronic structure and reactivity of transition and noble metals, Journal of Molecular Catalysis A: Chemical 115 (3) (1997) 421–429. doi:10.1016/S1381-1169(96)00348-2.

[12] S. Schnur, A. Groß, Strain and coordination effects in the adsorption properties of early transition metals: A density-functional theory study, Phys. Rev. B 81 (3) (2010) 033402–1–033402–4. doi:10.1103/PhysRevB.81.033402.

[13] M. Gsell, P. Jakob, D. Menzel, Effect of Substrate Strain on Adsorption, Science 280 (1998) 717–720.

[14] A. Schlapka, M. Lischka, A. Groß, U. Käsberger, P. Jakob, Surface Strain versus Substrate Interaction in Heteroepitaxial Metal Layers: Pt on Ru(0001), Phys. Rev. Lett. 91 (1) (2003) 016101–1–016101–4. doi:10.1103/PhysRevLett.91.016101.

[15] P. Ochal, J. L. G. de la Fuente, M. Tsypkin, F. Seland, S. Sunde, N. Muthuswamy, M. Rønning, D. Chen, S. Garcia, S. Alayoglu, B. Eichhorn, CO stripping as an electrochemical tool for characterization of RuPt core-shell catalysts, J. Electroanal. Chem. 655 (2) (2011) 140–146. doi:10.1016/j.jelechem.2011.02.027.

[16] M. Tsypkin, J. L. G. de la Fuente, S. G. Rodríguez, Y. Yu, P. Ochal, F. Seland, O. Safonova, N. Muthuswamy, M. Rønning, D. Chen, S. Sunde, Effect of heat treatment on the electrocatalytic properties of nano-structured Ru cores with Pt shells, J. Electroanal. Chem. 704 (2013) 57–66. doi:10.1016/j.jelechem.2013.06.007.

[17] J. C. Davies, J. Bonde, A. Logadóttir, J. K. Nørskov, I. Chorkendorff, The Ligand Effect:CO Desorption from Pt/Ru Catalysts, Fuel Cells 5 (4) (2005) 429–435. doi:10.1002/fuce.200400076.

[18] A. Jackson, V. Viswanathan, A. J. Forman, A. H. Larsen, J. K. Nørskov, T. F. Jaramillo, Climbing the Activity Volcano: CoreShell RuPt Electrocatalysts for Oxygen Reduction, ChemElectroChem 1 (1) (2014) 67–71. doi:10.1002/celc.201300117.

[19] L. Yang, M. B. Vukmirovic, D. Su, K. Sasaki, J. A. Herron, M. Mavrikakis, S. Liao, R. R. Adzic, Tuning the Catalytic Activity of RuPt CoreShell Nanoparticles for the Oxygen Reduction Reaction by Varying the Shell Thickness, J. Phys. Chem. C 117 (4) (2013) 1748–1753. doi:10.1021/jp309990e.

[20] S. Alayoglu, A. U. Nilekar, M. Mavrikakis, B. Eichhorn, RuPt coreshell nanoparticles for preferential oxidation of carbon monoxide in hydrogen, Nat. Mater. 7 (4) (2008) 333–338. doi:10.1038/nmat2156.

[21] H. Hoster, A. Schlapka, P. Gazdzicki, Oxygen Adsorption on Pt/Ru(0001) layers, J. Chem. Phys. 314 (2011) 224707–1 – 224707–10. doi:10.1063/1.3598957.

[22] F. Calle-Vallejo, D. Loffreda, M. T. M. Koper, P. Sautet, Introducing structural sensitivity into adsorption-energy scaling relations by means of coordination numbers, Nat. Chem. 7 (2015) 403–410. doi:10.1038/nchem.2226.

[23] A. A. Peterson, L. C. Grabow, T. P. Brennan, B. Shong, C. Ooi, D. M. Wu, C. W. Li, A. Kushwaha, A. J. Medford, F. Mbuga, L. Li, J. K. Nørskov, Finite-Size Effects in O and CO Adsorption for the Late Transition Metals, Top. Cat. 55 (19) (2012) 1276–1282. doi:10.1007/s11244-012-9908-x.

[24] A. Kulkarni, S. Siahrostami, A. Patel, J. K. Nørskov, Understanding Catalytic Activity Trends in the Oxygen Reduction Reaction, Chem. Rev. 118 (2018) 2302–2312. doi:10.1021/acs.chemrev.7b00488.

[25] R. Gómez, José, M. Orts, B. Álvarez Ruiz, J. M. Feliu, Effect of temperature on hydrogen adsorption on Pt(111), Pt(110), and Pt(100) electrodes in 0.1 m $HClO_4$, J. Phys. Chem. B 108 (2004) 228 – 238.

[26] K. Kinoshita, Electrochemical Oxygen Technology, John Wiley & Sons, Inc., 1992.

[27] K. Kinoshita, Particle size effects for oxygen reduction on highly dispersed platinum in acid electrolytes, J. Electrochem. Soc. 137 (1990) 845–848.

[28] S. Alayoglu, P. Zavalij, B. Eichhorn, Q. Wang, A. I. Frenkel, P. Chupas, Structural and Architectural Evaluation of Bimetallic Nanoparticles: A Case Study of Pt-Ru Core-Shell and Alloy Nanoparticles, ACS Nano 3 (10) (2009) 3127–3137. doi:10.1021/nn900242v.

[29] E. N. E. Sawy, H. A. El-Sayed, V. I. Birss, Novel electrochemical fingerprinting methods for the precise determination of Pt-shell coverage on Ru-core nanoparticles , Chem. Commun. 50 (2014) 11558–11561. doi:10.1039/c4cc04824e.

[30] K. J. J. Mayrhofer, B. B. Blizanac, M. Arenz, V. R. Stamenkovic, P. N. Ross, N. M. Marković, The Impact of Geometric and Surface Electronic Properties of Pt-Catalysts on the Particle Size Effect in Electrocatalysis, J. Phys. Chem. B 109 (30) (2005) 14433–14440. doi:10.1021/jp051735z.

[31] J. M. Feliu, E. Herrero, V. Climent, Electrocatalytic properties of stepped surfaces, in: E. Santos, W. Schmickler (Eds.), Catalysis in Electrochemistry: From Fundamentals to Strategies for Fuel Cell Development, John Wiley & Sons, Hoboken, New Jersey, 2011, Ch. 4, pp. 127 – 163.

[32] O. A. Petrii, Zero Charge Potentials of Platinum Metals and Electron Work Functions (Review), Russ. J. Electrochem. 49 (5) (2013) 401–422. doi:10.1134/S1023193513050145.

[33] A. Frumkin, O. A. Petrii, B. Damaskin, The notion of the electrode charge and the Lippmann equation, J. Electroanal. Chem. 27 (1) (1970) 81–100. doi:10.1016/S0022-0728(70)80204-2.

[34] V. Climent, J. M. Feliu, Thirty years of platinum single crystal electrochemistry, J. Solid State Electrochem. 15 (2011) 1297–1315. doi:10.1007/s10008-011-1372-1.

[35] S. Trasatti, E. Lust, The potential of zero charge, in: R. White, J. O. Bockris, B. Conway (Eds.), Modern Aspects of Electrochemistry No. 33, Kluwer Academic Publishers, New York, 1999, p. 1.

[36] C. Korzeniewski, V. Climent, J. M. Feliu, Electrochemistry at Platinum Single Crystal Electrodes, in: A. J. Bard, C. Zoski (Eds.), Electroanalytical Chemistry – A Series of Advances, Vol. 24, CRC Press, Boca Raton, 2012, Ch. 2, pp. 75–169.

[37] M. Weaver, Potentials of Zero Charge for Platinum(111)-Aqueous Interfaces: A Combined Assessment from In-Situ and Ultrahigh-Vacuum Measurements, Langmuir 14 (1998) 3932–3936.

[38] J. O. Bockris, A. K. N. Reddy, M. Gamboa-Aldeco, Modern Electrochemistry 2A: Fundamentals of Electrodics, 2nd Edition, Kluwer Academic Publishers, New York, 2000.

[39] A. N. Frumkin, O. A. Petrii, Potentials of zero total and zero free charge of platinum group metals, Electrochim. Acta 20 (5) (1975) 347–359. doi:10.1016/0013-4686(75)90017-1.

[40] Y. Garsany, O. A. Baturina, K. E. Swider-Lyons, S. S. Kocha, Experimental methods for quantifying the activity of platinum electrocatalysts for the oxygen reduction reaction, Anal. Chem. 82 (15) (2010) 6321–6328. doi:10.1021/ac100306c.

[41] Y. Garsany, J. Ge, J. St-Pierre, R. Rocheleau, K. E. Swider-Lyons, Analytical procedure for accurate comparison of rotating disk electrode results for the oxygen reduction activity of Pt/C, J. Electrochem. Soc. 161 (5) (2014) F628–F640. doi:10.1149/2.036405jes.

[42] V. Climent, R. Gomez, J. M. Orts, A. Rodes, A. Aldaz, J. M. Feliu, Interfacial Electrochemistry, Marcel Dekker, New York, 1999.

[43] D. van der Vliet, D. S. Strmcnik, C. Wang, V. R. Stamenkovic, N. M. Marković, M. T. M. Koper, On the importance of correcting for the uncompensated Ohmic resistance in model experiments of the Oxygen Reduction Reaction, J. Electroanal. Chem. 647 (1) (2010) 29–34. doi:10.1016/j.jelechem.2010.05.016.

[44] S. T. Briskeby, Carbon-Nano-Fibre Supported Electrocatalysts for Fuel Cells, Ph.D. thesis, Norwegian University of Science and Technology (2012).

[45] T.-Y. Jeon, K.-S. Lee, S. J. Yoo, Y.-H. Cho, S. H. Kang, Y.-E. Sung, Effect of surface segregation on the methanol oxidation reaction in carbon-supported Pt-Ru alloy nanoparticles, Langmuir 26 (11) (2010) 9123–9129. doi:10.1021/la9049154.

[46] M. Bernechea, S. García-Rodríguez, P. Terreros, E. de Jesús, J. L. G. Fierro, S. Rojas, Synthesis of Core-Shell PtRu Dendrimer-Encapsulated Nanoparticles. Relevance as Electrocatalysts for CO Oxidation, J. Phys. Chem. 115 (2011) 1287 – 1294.

[47] D.-J. Chen, A. M. Hofstead-Duffy, I.-S. Park, D. O. Atienza, C. Susut, S.-G. Sun, Y. Y. Tong, Identification of the Most Active Sites and Surface Water Species: A Comparative Study of CO and Methanol Oxidation Reactions on Core-Shell MPt (M = Ru, Au) Nanoparticles by in Situ IR Spectroscopy, Journal of Physical Chemistry C 115 (2011) 8735–8743. doi:10.1021/jp200557m.

[48] A. Jackson, A. Strickler, D. Higgins, T. F. Jaramillo, Engineering Ru@Pt Core-Shell Catalysts for Enhanced Electrochemical Oxygen Reduction Mass Activity and Stability, Nanomaterials

38 (2018) 1–15. doi:10.3390/nano8010038.

[49] N. R. Elzović, B. M. Babić, N. V. Kristajić, L. M. Vračar, Specificity of the UPD of H to the structure of highly dispersed Pt on carbon support, Int. J. Hydrogen Energy 32 (2007) 1991 – 1998.

[50] J. Clavilier, R. Alabat, R. Gomez, J. M. Orts, J. M. Feliu, A. Aldaz, CO-stripping at ru nanoparticles, J. Electroanal. Chem. 330 (1992) 489 – 497.

[51] R. Rizo, E. Sitta, E. Herrero, V. Climent, J. M. Feliu, Towards the understanding of the interfacial pH scale at Pt(111) electrodes, Electrochimica Acta 162 (2015) 138 – 145.

[52] R. Martínez-Hincapié, P. Sebastián-Pascual, V. Climent, J. M. Feliu, Investigating Interfacial Parameters with Platinum Single Crystal Electrodes, Russ. J. Electrochem. 53 (2017) 227–236.

[53] A. Ganassin, P. Sebastián, V. Climent, W. Schuhmann, A. S. Bandarenka, J. Feliu, On the pH Dependence of the Potential of Maximum Entropy of Ir(111) Electrodes, Scientific Reporst 7 (2017) 1246–1–1246–14. doi:10.1038/s41598-017-01295-1.

[54] M. E. Orazem, B. Tribollet, Electrochemical Impedance Spectroscopy, 2nd Edition, John Wiley & Sons, Hoboken (NJ), 2017.

[55] J. Newman, Resistance for flow of current to a disk, J. Electrochem. Soc. 113 (1966) 501 – 502.

[56] M. Tjelta, S. Sunde, Current-distribution effects on the impedance of porous electrodes and electrodes covered with films, J. Electroanal. Chem. 737 (2015) 65–77. doi:10.1016/j.jelechem.2014.09.030.

[57] K. J. J. Mayrhofer, D. Strmcnik, B. B. Blizanac, V. R. Stamenkovic, M. Arenz, N. M. Marković, Measurement of oxygen reduction activities via the rotating disc electrode method: From Pt model surfaces to carbon-supported high surface area catalysts, Electrochim. Acta 53 (7) (2008) 3181–3188. doi:10.1016/j.electacta.2007.11.057.

[58] A. López-Cudero, J. Solla-Gullón, E. Herrero, A. Aldaz, J. M. Feliu, CO electrooxidation on carbon supported platinum nanoparticles: Effect of aggregation, J. Electroanal. Chem. 644 (2) (2010) 117–126. doi:10.1016/j.jelechem.2009.06.016.

[59] F. Maillard, S. Schreier, M. Hanzlik, E. R. Savinova, S. Weinkauf, U. Stimming, luence of particle agglomeration on the catalytic activity of carbon-supported Pt nanoparticles in CO monolayer oxidation, Phys. Chem. Chem. Phys. 7 (2) (2005) 385–393. doi:10.1039/B411377B.

[60] S. W. T. Price, J. M. Rhodes, L. Calvillo, A. E. Russell, Revealing the Details of the Surface Composition of Electrochemically Prepared AuPd CoreShell Nanoparticles with in Situ EXAFS, J. Phys. Chem. C 117 (2013) 24858–24865.

[61] U. A. Paulus, T. J. Schmidt, H. A. Gasteiger, R. J. Behm, Oxygen reduction on a high-surface area Pt/Vulcan carbon catalyst: a thin-film rotating ring-disk electrode study, J. Electroanal. Chem. 495 (2) (2001) 134–145. doi:10.1016/S0022-0728(00)00407-1.

[62] M. Montiel, P. Hernández-Fernández, J. L. G. Fierro, S. Rojas, P. Ocón, Promotional effect of upper Ru oxides as methanol tolerant electrocatalyst for the oxygen reduction reaction, J. Power Sources 191 (2) (2009) 280–288. doi:10.1016/j.jpowsour.2009.02.023.

[63] D. Bokach, J. L. G. de la Fuente, M. Tsypkin, P. Ochal, I. C. Endsjø, R. Tunold, S. Sunde, F. Seland, High-Temperature Electrochemical Characterization of Ru Core Pt Shell Fuel Cell Catalyst, Fuel Cells 11 (6) (2011) 735–744. doi:10.1002/fuce.201000187.

[64] M. T. M. Koper, T. J. Schmidt, N. M. Marković, P. N. Ross, Potential Oscillations and S-shaped Polarization Curve in the Continuous Electro-oxidation of CO on Platinum Single-crystal Electrodes, J. Phys. Chem. B 105 (35) (2001) 8381–8386. doi:10.1021/jp011410s.

[65] J. Svendby, F. Seland, M. Jensen, S. Sunde, In Preparation.

[66] T. Holm, P. K. Dahlstrøm, S. Sunde, F. Seland, D. A. Harrington, Dynamic electrochemical impedance study of methanol oxidation at Pt at elevated temperatures, Electrochimica Acta XXX (2018) yy–yy.

[67] B. Conway, J. Barber, S. Morin, Comparative evaluation of surface structure specifcity of kinetics of UPD and OPD of H at single-crystal Pt electrodes, Electrochimica Acta 44 (1998) 1109–1125.

[68] K. J. P. Schouten, M. J. T. C. van der Niet, M. T. M. Koper, Impedance spectroscopy of H and OH adsorption on stepped single-crystal platinum electrodes in alkaline and acidic media, Physical Chemistry Chemical Physics 12 (2010) 15217–15224. doi:10.1039/c0cp00104j.

[69] G. A. Attard, A. Brew, K. Hunter, J. Sharman, E. Wright, Specific adsorption of perchlorate anions on Pt{hkl} single crystal electrodes, Phys.Chem.Chem.Phys. 16 (2014) 13689 – 13698.

[70] Y.-F. Huang, P. J. Kooyman, M. T. M. Koper, Intermediate stages of electrochemical oxidation of single-crystalline platinum revealed by in situ Raman spectroscopy, Nature Communicationsdoi:10.1038/ncomms12440.

[71] H. Hoster, B. Richter, R. J. Behm, Catalytic Influence of Pt Monolayer Islands on the Hydrogen Electrochemistry of Ru(0001) Studied by Ultrahigh Vacuum Scanning Tunneling Microscopy and Cyclic Voltammetry, J. Phys. Chem. B 108 (2004) 14780–14788. doi:10.1021/jp047576l.

[72] P. Jakob, A. Schlapka, P. Gazdzicki, Oxygen adsorption on Pt/Ru(0001) layers, J. Chem. Phys. 134 (2011) 224707. doi:10.1063/1.3598957.

[73] R. V. Hardeveld, F. Hartog, The Statistics of Surface Atoms and Surface Sites on Metal Crystals, Surf. Sci. 15 (1969) 189–230.

[74] G. Cao, Nanostructures & Nanomaterials. Synthesis, Properties, and Applications, Imperial College Press, London, 2004.

[75] A. W. Adams, A. P. Gast, Physical Chemistry of Surfaces, 6th Edition, John Wiley & Sons, New York, 1997.